

Binding Energy and Intermolecular Vibrations of Neutral and Ionized *p*-Fluorotoluene·Ar Cluster by Mass Analyzed Threshold Ionization

S. Georgiev, T. Chakraborty,[†] and H. J. Neusser*

Institut für Physikalische und Theoretische Chemie, Technische Universität München, Lichtenbergstrasse 4, D-85748 Garching, Germany

Received: September 30, 2003; In Final Form: January 22, 2004

The binding energies in the neutral and ionic ground states of the *p*-fluorotoluene·Ar (*p*FT·Ar) van der Waals complex have been measured by the use of the mass analyzed threshold ionization (MATI) technique. The breakdown of the parent ion signal and the simultaneous detection of threshold ions at the fragment mass when the internal energy of the threshold cluster ion is increased above the dissociation limit are used as a probe for determining the cluster binding energy. The necessary density of vibrational bands in the vicinity of the dissociation threshold is achieved by excitation via the 9b¹₀ band in a resonance enhanced two-photon excitation process. We find a strong Franck–Condon activity of the asymmetric bending vibrations pointing to a geometrical change of the Ar position along the long (*x*) molecular axis because of a charge shift along this axis after ionization.

1. Introduction

van der Waals (vdW) complexes (clusters) consisting of an aromatic compound and rare-gas atoms allow us to investigate “weak” intermolecular interactions, which play a significant role in a great variety of physical, chemical, and biological processes¹. *p*-Fluorotoluene·Ar (*p*FT·Ar) is an interesting system for investigation of these weak interactions as both the fluorine and methyl groups can have an additive influence on the overall van der Waals binding with the Ar atom. The influence only of F on the Ar position has been demonstrated for fluorobenzene·Ar with high-resolution UV and microwave spectroscopy.^{2,3} Up to now, *p*FT has been studied by the following spectroscopic methods: zero kinetic electron energy (ZEKE) spectroscopy⁴ and resonance enhanced multiphoton photoionization (REMPI).⁵ Here we present results from mass analyzed threshold ionization (MATI) applied for the first time to this cluster. MATI is a useful tool for investigating the dissociation of weakly bound cluster ions of large polyatomic molecules to which such methods as high-pressure mass spectrometry,⁶ IR absorption spectroscopy in gas mixtures,⁷ or bolometric methods⁸ have not been yet applied. The determination of the binding energy (BE) of the clusters is of particular interest as BE values are important microscopic parameters for the description of the properties of condensed matter.

The MATI technique is based on the existence of long-lived high Rydberg states in the vicinity of different ionization thresholds.^{9,10} The essence of the technique has been described in the literature;^{11,12} therefore, only salient features of the method are described here.

The studied systems (atoms, molecules, and clusters) are excited to Rydberg states close below to the respective vibrational eigenstate of the ion. It is well-known that for every state of the ion there is a Rydberg series converging to it.

Furthermore, it is assumed that the interaction of the high Rydberg electron and the positively charged ionic core is described accurately enough with a Coulomb potential, so the high Rydberg states are located close to the respective ionization energy and their series limits denote the energetic position of the rovibrational eigenstates of the ionic core with high precision. The weakly bound Rydberg electrons are detached from the ionic cores by applying a pulsed electric field. Then the threshold ions produced in this way are detected and monitored as a function of the ionizing laser wavelength in a time-of-flight (TOF) mass spectrometer.¹² This enables one to observe mass changes due to fragmentation processes of the studied cluster ion system as a function of the internal energy. The dissociation of a cluster ion in its ground electronic state is precisely monitored by a simultaneous observation of threshold ions in the cluster (parent) channel and the fragment (daughter) channel. However, there are two main preconditions for the unambiguous determination of the dissociation threshold. First, there must exist ionic vibrational states closely below and above the field free dissociation threshold.¹⁰ This might be a problem for the sparse vibronic spectrum in this work when using a single intermediate state in the two-photon excitation process. Here we solve this problem by choosing a suitable intermediate state leading to a dense vibrational state spectrum in the dissociation region of the cluster ion. Another requirement for the determination of the dissociation threshold is that the S₁ ← S₀, 0⁰₀ vibronic bands of the monomer and the cluster are narrow and differ sufficiently in their frequencies so that they can be excited separately. This is the case for the *p*-fluorotoluene·Ar cluster, studied in this work.

After the binding energy of the ground cationic state is found from the experiment, the binding energy of the ground neutral state of the cluster can be determined if the adiabatic ionization energies of the monomer and the cluster are known.¹⁰

2. Experimental Section

Our experimental setup for measuring the MATI spectra of molecules and clusters has been described before in detail.¹²

* To whom correspondence should be addressed. E-mail: neusser@ch.tum.de.

[†] Present address: Department of Chemistry, Indian Institute of Technology Kanpur, UP-208016 India.

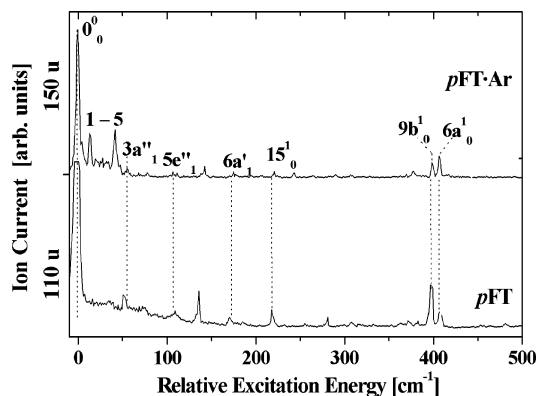


Figure 1. $S_1 \leftarrow S_0$ REMPI two color spectra of *p*-fluorotoluene (lower trace) and *p*-fluorotoluene·Ar cluster (upper trace). Both spectra are displayed on a common relative excitation energy scale, normalized to the 0_0^0 origin frequency. The position of the origins for *p*FT and *p*FT·Ar are $36\,860\text{ cm}^{-1}$ and $36\,825\text{ cm}^{-1}$, respectively. For details, see the text.

Briefly, the setup consists of two dye lasers (FL 3002 and LPD 3000; Lambda Physik), which are synchronously pumped by a XeCl excimer laser (EMG 1003i, Lambda Physik) to generate tunable light pulses of ~ 10 ns duration and spectral bandwidth $\sim 0.3\text{ cm}^{-1}$. The two counterpropagating laser beams overlap collinearly in the vacuum chamber, and they intersect a skimmed supersonic molecular beam perpendicularly 15 cm downstream the nozzle orifice.

The cold molecular beam is obtained by supersonic expansion of a gas mixture (consisting of *p*-fluorotoluene and Ar) into the vacuum. The light pulses overlap in time and space in the center of the first stage of a double stage acceleration configuration of the ion optics of a time-of-flight mass spectrometer, formed by three metal disks with holes.¹² One of the lasers is tuned to a vibronic band in the $S_1 \leftarrow S_0$ transition of the *p*-fluorotoluene (*p*FT) monomer or *p*-fluorotoluene·Ar cluster, respectively. The other one is tuned to a transition from this intermediate state to high Rydberg states. The Rydberg molecules are separated from the directly produced photoions in the first stage by a weak electric field (about $0.2\text{--}0.6\text{ V/cm}$) and are field-ionized by applying a strong electric field of 1000 V/cm in the second stage. The resulting ions are accelerated and injected by the same electric field into a linear TOF mass spectrometer. The detected signals at two different mass channels (cluster parent mass and monomer fragment mass) are recorded simultaneously with two gated integrators, then digitized, and processed in a personal computer.

3. Results and Discussion

3.1. REMPI Spectra. Using REMPI two-color technique, we first examined the S_1 electronic intermediate state of *p*FT and *p*FT·Ar. In Figure 1, the spectra of *p*FT (lower trace) and *p*FT·Ar (upper trace) are shown. The origin band of the S_1 state is located at $36\,860 \pm 5\text{ cm}^{-1}$ for the monomer and at $36\,825 \pm 5\text{ cm}^{-1}$ for the *p*FT·Ar cluster. Thus, the $S_1 \leftarrow S_0$, 0_0^0 band of the latter is red shifted to that of the former by about 35 cm^{-1} . This value is in good agreement with that reported by Hu et al.⁵ It is larger than the one obtained for the fluorobenzene·Ar cluster (24 cm^{-1})¹³ and for toluene·Ar (23 cm^{-1}).¹⁴ In the low-frequency region (close to the origin band) of the *p*FT·Ar complex along with the CH_3 rotational bands we were able to identify bending vibrations of the *p*FT·Ar cluster in agreement with Hu et al.⁵ (see Figure 1, where these bands are indicated by numbers). The peaks originating from internal rotation of the CH_3 group are assigned following refs 15–17.

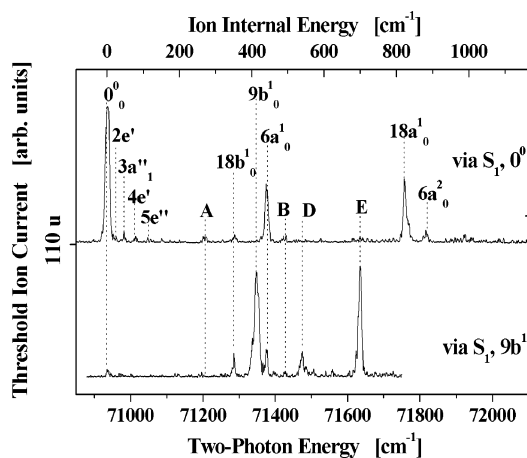


Figure 2. MATI spectra of *p*-fluorotoluene via $S_1, 0^0$ (upper trace) and $S_1, 9b^1$ (lower trace) intermediate states. For more details, see the text and Table 1.

3.2. MATI Spectra. As a next step in our experiments, we recorded MATI spectra of *p*FT and *p*FT·Ar choosing two different intermediate states in both the cases – the vibrationless origin of $S_1, 0^0$ (a_1 symmetry) and the $S_1, 9b^1$ vibronic state ($A_1 \otimes b_1 = B_1$ symmetry),^{15,18} which is located at 398 cm^{-1} (see Figure 2) above the origin. This state corresponds to the first quantum of a ring vibration.¹⁹ Our measurements suggest that the values for the adiabatic ionization energies (AIE) of the monomer and the *p*FT·Ar cluster are $70\,935 \pm 5\text{ cm}^{-1}$ and $70\,754 \pm 5\text{ cm}^{-1}$, respectively. Thus, the AIE of the *p*FT·Ar cluster is 181 cm^{-1} red shifted from that of *p*FT monomer. This value of AIE shift is smaller than what has been observed before for the fluorobenzene·Ar cluster (222 cm^{-1})¹³ but larger than in the case of the toluene·Ar cluster (161 cm^{-1}).¹⁴ In Figure 2, we present MATI spectra for *p*FT measured via the two intermediate states, $S_1, 0^0$ (upper trace) and $S_1, 9b^1$ (lower trace). The peaks corresponding to internal rotations of the CH_3 group are designated according to Takazawa et al.⁴ The assignments for the peaks at 440 , 823 , and 883 cm^{-1} are made by comparison with the results for fluorobenzene⁺ by Lembach et al.²⁰ The peak at 413 cm^{-1} (see Figure 2) has been assigned to the $9b$ vibration of the *p*FT cation, and it appears with a slightly higher frequency than the $9b$ vibration in the neutral S_1 state (398 cm^{-1}). Comparing the two spectra in Figure 2, we find the following features: (i) the intensity of the 0_0^0 peak is much weaker when exciting the molecule via the $S_1, 9b^1$ than via the $S_1, 0^0$ state, (ii) some of the bands which are very weak in intensity in the first case (via $S_1, 0^0$) are very strong in the other case (via $S_1, 9b^1$), e.g., $18b^1_0$ and D bands, and vice versa, e.g., $6a^1_0$ band, and (iii) new bands are present in the spectrum when exciting via $S_1, 9b^1$ state. All these findings are consequences of the different Franck–Condon factors for ionization from the two intermediate states. The peaks at 540 (peak D) and 701 cm^{-1} (peak E) are due to vibrations of the ion containing $9b$ character (i.e., a bending motion of the F atom and the CH_3 group, e.g., the ν_3 vibration) so that the Franck–Condon factors for their excitation in the second absorption step are large. The discussed bands are also listed in Table 1.

3.3. Dissociation of the (*p*FT·Ar)⁺ Cluster. In Figure 3 in addition to the MATI spectrum of *p*FT⁺ (lower trace), the MATI spectrum of the (*p*FT·Ar)⁺ cluster is presented (upper trace) on a common excess energy scale above the respective AIE. Both spectra are obtained by exciting the respective vibrationless origin $S_1, 0^0$ as an intermediate state. The band positions in the (*p*FT·Ar)⁺ spectrum agree quite well with the corresponding

TABLE 1: Bands, Observed in the Threshold Ion (MATI) Spectra of *p*-Fluorotoluene via $S_1,0^0$ and $S_1,9b^1$ Intermediate States (see also Figure 2)^a

band	2e'	3a ₁ ⁻	4e'	5e ⁻	A	18b ₀ ¹	9b ₀ ¹	6a ₀ ¹	B	D	E	18a ₀ ¹	6a ₀ ²
excess energy [cm ⁻¹]	22	52	79	121	269	356	413	440	491	540	701	823	883

^a Excess energies are given in cm⁻¹ above the 0⁰ level of the ground state of the *p*-fluorotoluene cation.

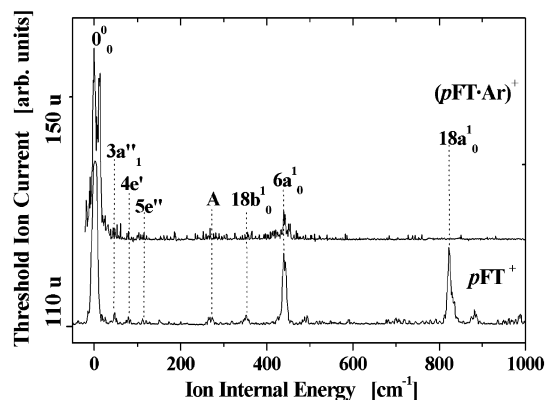


Figure 3. MATI spectra of *p*-fluorotoluene (lower trace) and *p*-fluorotoluene·Ar (upper trace) via the corresponding origin band. Both spectra are presented on a common excess energy scale. The positions of the adiabatic ionization thresholds for *p*-fluorotoluene and *p*-fluorotoluene·Ar are 70 935 and 70 754 cm⁻¹, respectively. For details, see the text.

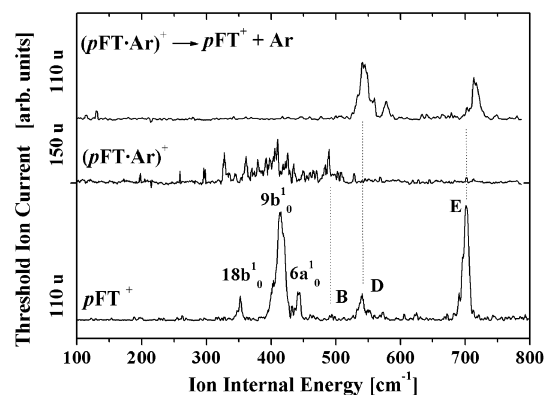


Figure 4. MATI spectra via $S_1,9b^1$ intermediate state of *p*-fluorotoluene recorded at 110 u (lower trace) and of *p*-fluorotoluene·Ar recorded at 150 u (middle trace) and 110 u (upper trace), showing a dissociation of the *p*-fluorotoluene·Ar cluster. All spectra are presented on a common excess energy scale. For explanations, see the text.

ones in the monomer spectrum and can thus be identified up to the strong 6a₀¹ band. The striking difference between the two spectra is the disappearance of the bands in the cluster ion spectrum in the excess energy region above the 6a₀¹ band (440 cm⁻¹). The reason for the breakdown of the signal is due to the dissociation of the (*p*FT·Ar)⁺ cluster. However, the monomer spectrum in the case of excitation via the S_1 origin is not rich in bands in the region between 500 and 700 cm⁻¹. This is a significant drawback, since the dissociation of (*p*FT·Ar)⁺ is expected in this region as reported for clusters of other organic molecules with Ar.^{10,12,13} A solution for this problem is to use the $S_1 \leftarrow S_0, 9b^1_0$ transition rather than the origin band for excitation, since in this case the region of interest is rich in bands as can be seen from Figure 2 (lower trace). The excitation of the nearby somewhat stronger, 6a₀¹ vibrational state would lead to a MATI spectrum with the same peaks in the dissociation region as in Figure 3 because the 6a₀¹ vibration is totally symmetric.

Figure 4 shows the MATI spectra measured via the 9b₀¹ intermediate state. The upper and the middle traces represent

TABLE 2: Electronic Origins of $S_1 \leftarrow S_0$ Transitions and the AIEs of *p*-Fluorotoluene and the *p*-Fluorotoluene·Ar Cluster^a

	$S_1 \leftarrow S_0, 0^0_0$ [cm ⁻¹]	IE [cm ⁻¹]	E_0 [cm ⁻¹]	D_0 [cm ⁻¹]
<i>p</i> FT	36 860 ± 5	70 935 ± 5		
<i>p</i> FT·Ar	36 825 ± 5	70 754 ± 5	510 ± 20	329 ± 20

^a Binding energies in the ground ionic (E_0) and ground neutral (D_0) states for the *p*-fluorotoluene·Ar cluster are also given.

the MATI cluster spectra measured at the daughter (110 u) and the parent mass (150 u) channel, respectively, when exciting the 9b₀¹ band of the *p*FT·Ar cluster at 37 223 cm⁻¹. The lowest trace represents the MATI spectrum of *p*FT measured at 110 u when tuning the first laser frequency to the 9b₀¹ band of the monomer at 37 258 cm⁻¹. The horizontal scale is given in common excess energy units above the AIE for the three traces. As it can be seen from Figure 4, the spectral pattern measured at the parent mass channel of the cluster (middle trace) follows the pattern in the spectrum of the directly excited monomer up to band B at 491 cm⁻¹ above the AIE, even though the signal-to-noise ratio in the middle trace (cluster spectrum) does not allow to identify each detail in the band structure seen in the lowest trace (monomer spectrum). The signal in the middle trace disappears around 510 cm⁻¹. There is no band directly seen at this position in the lowest trace but several weak bands (e.g., intermolecular vibrations) may be overlapping in this region leading to unstructured background. On the other hand, peak D is clearly appearing in the fragment mass spectrum (top trace) and no longer present in the parent ion spectrum (middle trace).

We take the disappearance of the cluster ion signal as the dissociation threshold and obtain the ionic binding energy $E_0 = 510 \pm 20$ cm⁻¹ according to a procedure described in our previous work for the fluorobenzene·Ar cluster.¹³ Thus, we can directly compare the values for the dissociation threshold reported in this work with that of fluorobenzene·Ar. The value for E_0 is somewhat smaller than that of 568 cm⁻¹ obtained for the fluorobenzene·Ar cluster.¹³ Using the measured values for the AIEs both of *p*FT·Ar and *p*FT, the binding energy D_0 of the neutral cluster is calculated from the relation $D_0 = E_0 + \text{AIE}(\text{cluster}) - \text{AIE}(\text{monomer})$.¹² Its value $D_0 = 329 \pm 20$ cm⁻¹ is close to that of fluorobenzene·Ar (346 ± 10 cm⁻¹).¹³ From our results, we conclude that the presence of the methyl group does not influence the vdW bonding by dispersion interaction, located above the plane of the neutral aromatic ring. In the ionized cluster, however, there is a stronger contribution from charge-induced interaction in fluorobenzene·Ar than in *p*FT·Ar. Table 2 gives a summary for the positions of the origins of S_1 , AIEs for and *p*FT and *p*FT·Ar cluster as well as the binding energies in the ground ionic (E_0) and ground neutral (D_0) states for the *p*FT·Ar.

3.4. Intermolecular Bands. A closer inspection of the spectra in Figure 4 reveals a small shift of the relative frequency position of band E in the cluster spectrum (top trace), compared to the corresponding one in the monomer spectrum. There are two possible explanations for this finding: (i) the Ar atom has an effect on the internal rotations of the CH₃ group, enhancing transitions to higher internal rotational levels of the correspond-

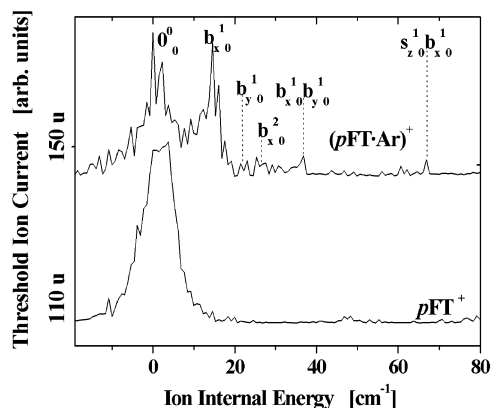


Figure 5. MATI spectra of *p*-fluorotoluene (lower trace) and *p*-fluorotoluene·Ar (upper trace) in the vicinity of the adiabatic ionization threshold. Both spectra are displayed on a common excess energy scale. For details, see the text.

ing vibrational state for some bands⁵ and (ii) intermolecular vibrational levels are excited. To clarify this point, we measured the AIE origin of pFT^+ and $(pFT \cdot Ar)^+$ cations under improved resolution yielding the spectra shown in Figure 5. The $(pFT \cdot Ar)^+$ spectrum has an interesting feature, namely the split profile of the AIE band unlike that of the monomer (see Figures 3 and 5). This splitting of 15 cm^{-1} , we believe, is due to excitation of the bending vibration b_x^1 of the Ar atom relative to the long axis of the aromatic ring. This value is close to that of the b_x vibration of the Ar atom in the S_1 state of the cluster (13 cm^{-1} as reported in the literature,⁵ see Figure 1). The smaller peaks in Figure 5 at higher energy are then tentatively assigned to b_y^1 , b_x^2 , b_x^1 , b_y^1 , and s_z^1 b_x^1 bending vibrations by comparison with the intermolecular frequencies in S_1 reported by Hu et al.⁵ There is an additional structure within the individual bands with a peak spacing of about 2 cm^{-1} in the MATI spectrum of $(pFT \cdot Ar)^+$ (upper trace in Figure 5) which is not present in the pFT^+ spectrum (lower trace in Figure 4). A similar structure even less pronounced with a spacing of adjacent peaks of 1.5 cm^{-1} is found in the $S_1 \leftarrow S_0$, 0^0_0 band of the $(pFT \cdot Ar)$ cluster. Possible explanations are a rotational contour of the bands and more likely an additional splitting because of a perturbation of the internal rotation of the CH_3 group caused by the attached Ar atom.

The strong Franck Condon activity of the b_x vibration of the AIE origin band discussed above shows that the reason for the shift of the band E of $11 \pm 5 \text{ cm}^{-1}$ is the additional excitation of one quantum of the intermolecular bending vibration b_x^1 . Similar results for the excitation of additional quanta of the bending b_x^1 vibration were found in the MATI spectra of fluorobenzene·Ar¹³ and ZEKE spectra of aniline·Ar.²¹ The bending b_x vibration leads to a motion of the Ar along the C_2 axis of the pFT^+ molecular ion. The strong b_x^1 band in the $(pFT \cdot Ar)^+$ MATI spectrum indicates a significant geometrical change of the cluster along the x coordinate upon ionization. This may result from a charge shift along the x axis after ionization from the benzene ring to the F atom. As a consequence, the charge induced part of the intermolecular interaction present after ionization would have an x -dependence different from the dispersive attraction present in the neutral and the ionic clusters.

4. Summary and Conclusion

In this work, we present the binding energies of the neutral and ionic *p*-fluorotoluene·Ar cluster measured with the MATI technique. To achieve a sufficient accuracy, we have chosen the S_1 , $9b^1$ intermediate state in the resonance-enhanced two-photon excitation yielding a dense vibronic spectrum in the vicinity of the dissociation threshold of the cluster ion. The resulting binding energies are 510 (329) cm^{-1} for the ionic (neutral) $pFT \cdot Ar$ cluster. Although the binding energy of the neutral $pFT \cdot Ar$ is the same as in fluorobenzene·Ar, in the case of the ionic $(pFT \cdot Ar)^+$, it is smaller by 58 cm^{-1} than in (fluorobenzene·Ar)⁺. This points to a stronger charge induced interaction in the absence of the CH_3 group. The MATI spectra of $(pFT \cdot Ar)^+$ reveal a strong Franck–Condon activity of the b_x bending mode. This we explain by a shift of the Ar atom along the long (x) axis of the molecule after ionization demonstrating a noticeable contribution of charge-induced interaction to the intermolecular bending in the ionized $(pFT \cdot Ar)^+$ cluster. In conclusion, we have demonstrated that the MATI technique provides accurate binding energies of energy-selected clusters if a suitable intermediate state is chosen to increase the vibronic band density in the MATI spectrum around the dissociation threshold.

It is highly desirable to calculate the binding energies of the neutral and ionic forms of fluorobenzene·Ar and $pFT \cdot Ar$ complexes by ab initio theoretical methods and compare the results with our experimental data for a better understanding of the effect of methyl substitution on van der Waals binding. Works in this direction are in progress.

Acknowledgment. The authors thank Dr. Julian Braun for valuable discussions. Financial support from the Deutsche Forschungsgemeinschaft and the Fonds der Chemischen Industrie is gratefully acknowledged.

References and Notes

- (1) For a review, see: *Chem. Rev.* **1994** entire volume.
- (2) van Herpen, W. M.; Meerts, W. L.; Dymannus, A. *Laser. Chem.* **1986**, *6*, 37.
- (3) Brupbacher, Th.; Bauder, A. *Chem. Phys. Lett.* **1990**, *173*, 435.
- (4) Takazawa, K.; Fujii, M.; Ito, M. *J. Chem. Phys.* **1993**, *99*, 3205.
- (5) Hu, Y.; Wang, X.; Yang, S. *Chem. Phys.* **2003**, *290*, 233.
- (6) Kemper, P. R.; Weis, P.; Bowers, M. T. *Int. J. Mass Spectrom. Ion Proc.* **1997**, *160*, 17.
- (7) Hunnicutt, S. S.; Branch, T. M.; Everhart, J. B.; Dudis, D. S. *J. Phys. Chem.* **1996**, *100*, 2083.
- (8) Oudejans, L.; Miller, R. E. *J. Phys. Chem. A* **1997**, *101*, 7582.
- (9) Zhu, L.; Johnson, P. M. *J. Chem. Phys.* **1991**, *94*, 5769.
- (10) Krause, H.; Neusser, H. J. *J. Chem. Phys.* **1992**, *97*, 5923.
- (11) Braun, J. E.; Neusser, H. J. *Mass Spectrom. Rev.* **2002**, *21*, 16.
- (12) Braun, J. E.; Mehnert, T.; Neusser, H. J. *Int. J. Mass Spectrom.* **2000**, *203*, 1.
- (13) Grebner, Th. L.; Unold, P. v.; Neusser, H. J. *J. Phys. Chem. A* **1997**, *101*, 158.
- (14) Eisenhardt, C. G.; Baumgärtel, H. *Ber. Bunsen-Ges. Phys. Chem.* **1998**, *102*, 12.
- (15) Okuyama, K.; Mikami, N.; Ito, M. *J. Phys. Chem.* **1985**, *89*, 5617.
- (16) Zhao, Z.; Parmenter, C. J. *J. Chem. Phys.* **1992**, *96*, 6362.
- (17) Ha, Y. M.; Choi, I. S.; Lee, S. K. *Bull. Korean Chem. Soc.* **1997**, *19*, 202.
- (18) Moss, D.; Parmenter, C.; Ewing, G. J. *J. Chem. Phys.*, **1987**, *86*, 51.
- (19) Brodersen, S.; Langseth, A. *Mater. Fys. Skr. Dan. Vid. Selsk* **1956**, *1*, 1.
- (20) Lembach, G.; Brutschy, B. *J. Phys. Chem.* **1996**, *100*, 19758.
- (21) Zhang, X.; Smith, J. M.; Knee, J. L. *J. Chem. Phys.* **1992**, *97*, 2843.